EARTH'S CRYOSPHERE
SCIENTIFIC JOURNAL

Earth's Cryosphere, 2022, vol. XXVI, No. 5, pp. 35–47

GASES AND GAS HYDRATES IN THE EARTH'S CRYOSPHERE

METHANE IN FROZEN AND THAWING SEDIMENTS OF WESTERN RUSSIAN ARCTIC

N.A. Zadorozhnaya[1,*], G.E. Oblogov[1,2], A.A. Vasiliev[1,2], I.D. Streletskaya[3], G.V. Malkova[1,2], P.B. Semenov[4], B.G. Vanshtein[4]

[1] *Earth Cryosphere Institute, Tyumen Science Center, Siberian Branch of the Russian Academy of Sciences, Malygina St. 86, Tyumen, 625026 Russia*
[2] *Tyumen State University, Volodarskogo St. 6, Tyumen, 625003 Russia*
[3] *Lomonosov Moscow State University, Faculty of Geography, Department of Cryolithology and Glaciology, Leninskie Gory 1, Moscow, 119991 Russia*
[4] *All-Russia Scientific Research Institute of Geology and Mineral Resources of the World Ocean (VNIIOkeangeologia), Angliiskii prosp. 1, St. Petersburg, 190121 Russia*

**Corresponding author; e-mail: z.nataliia.95@gmail.com*

The results of studies of the methane content in the active layer and upper permafrost horizon in the areas of the Marre-Sale station (western Yamal Peninsula) and the Pechora River mouth are presented. Data on the methane content in Quaternary permafrost and ground ice of different geneses and data on methane emission from the surface of typical tundra in Marre-Sale are analyzed. The highest methane content in sediments of both the active layer and the upper permafrost is characteristic of boggy floodplains and waterlogged depressions on the surface of the marine terrace. In well-drained landscapes, methane is virtually absent in sediments of the active layer. In the upper permafrost, its content is 5–6 times higher than in the overlying active layer. A large amount of methane (on average, about 2 mL/kg) is contained in loamy clay marine sediments at the base of the Marre-Sale section, as well as in the massive ice. The distribution of methane in permafrost and ground ice is close to a lognormal distribution. Significant methane flux (up to 10.7 mg/(m^2·h)) has been determined for highly moistened surfaces occupying about 45–50% of the area of a typical tundra.

Keywords: *methane, permafrost, transient layer, ground ice, methane emission, Marre-Sale, Pechora River mouth.*

Recommended citation: Zadorozhnaya N.A., Oblogov G.E., Vasiliev A.A., Streletskaya I.D., Malkova G.V., Semenov P.B., Vanshtein B.G., 2022. Methane in frozen and thawing sediments of Western Russian Arctic. *Earth's Cryosphere* **26** (5), 35–47.

INTRODUCTION

The greenhouse effect on climate change cannot be assessed without taking into consideration greenhouse gases emitted to the atmosphere from natural sources. Permafrost contains enormous reserves of greenhouse gases [*Rivkina et al., 1992; Sturtevant et al., 2012; Christensen, 2014; Schuur et al., 2015; Euskirchen et al., 2017; Streletskaya et al., 2018b; van Huissteden, 2020*]. The high content of greenhouse gases in permafrost is related to the considerable content of organic matter in the Quaternary sediments of the Arctic region. Greenhouse gases – methane CH_4 and carbon dioxide CO_2 – are produced in the course of microbial decomposition of organic matter. The warming potential of methane is at least 28 times higher than the warming potential of CO_2 (over 100 years) [*IPCC, 2018*]. Continuing warming in the Arctic [*IPCC, 2018*] may lead to the emission of greenhouse gases that are currently stored in permafrost and ground ice [*McCalley et al., 2014; Dean et al., 2018*].

According to available estimates, methane emissions from Arctic ecosystems, primarily from waterlogged and boggy areas, reach 8 to 29 Tg C/yr [*McGuire et al., 2012*], which corresponds to about 10% of the global CH_4 emission from natural wetlands [*Ciais et al., 2013*]. Some researchers believe that current estimates of CO_2 and CH_4 emissions caused by dramatic permafrost thawing may be underestimated [*Anthony et al., 2018*]. The point is that the greenhouse gas emissions increase due to the expansion of waterlogged areas and thermokarst lakes, where organic carbon becomes available for microbial decomposition [*van Huissteden, 2020*]. There is also an opposite opinion stating that the emission of greenhouse gases related to permafrost degradation is not so large and may not have a significant impact on climate change [*Anisimov, 2007*].

Copyrights © 2022 N.A. Zadorozhnaya, G.E. Oblogov, A.A. Vasiliev, I.D. Streletskaya, G.V. Malkova, P.B. Semenov, B.G. Vanshtein, All rights reserved.

Methane may have abiogenic, biogenic, thermogenic, and pyrogenic origins. Biogenic CH_4 is a final product of the organic matter decomposition by methanogenic archaea in the anaerobic environments, such as waterlogged soils, bogs, and marine sediments [*Streletskaya et al., 2018a*]. In typical tundras, the biogenic CH_4 is formed in the oxygen-free water-saturated active layer and in talik zones in the presence of sufficient amount of organic carbon in available forms [*Kraev et al., 2013; Kraev, Rivkina, 2017*].

It has been experimentally found that no methane is generated in frozen sediments [*Walz et al., 2017*], i.e., the entire amount of methane emitted from frozen sediments was formed before or during freezing and is a characteristic of host sediments themselves. The same can be stated for ground ice. The microbial activity in the active layer (AL) continues until the moment of its complete freezing [*Sturtevant et al., 2012*]. It has also been confirmed that a decrease in sediment temperatures reduces the activity of methane-oxidizing microbes in the upper horizons of the active layer [*Sachs et al., 2008*].

Field observations and experiments in the northeast of Siberia demonstrated that biogenic methane tends to accumulate near the lower boundary of the AL [*Kraev et al., 2017*]. During freezing, CH_4 may be squeezed out of this layer down into the permafrost for the first few meters and accumulate in lithological "pockets".

The aim of this study is to analyze factual data on the methane content in the AL and Quaternary permafrost, especially in the upper permafrost horizon (UPH), or the transient and intermediate layers according to Yu.L. Shur [*French, Shur, 2010*] and in the ground ice, as well as on the methane emission from the predominant landscapes of studied regions in the western sector of the Russian Arctic.

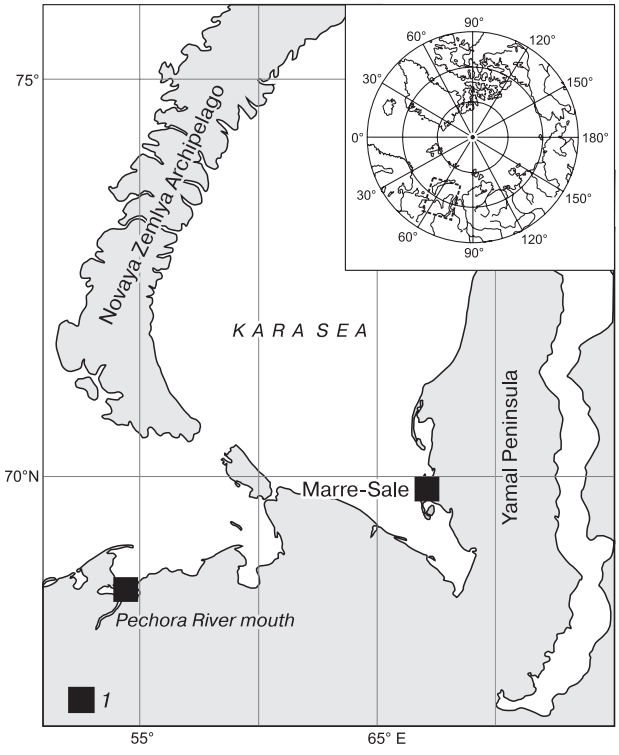

Fig. 1. Location of key sites.

1 – key site.

STUDY SITES

Long-term studies of the geological, geocryological, and landscape conditions have been performed in the areas of geocryological stations in the Yamal Peninsula (Marre-Sale) and the Pechora River mouth [*Pavlov et al., 2002; Kanevskii et al., 2005; Streletskaya et al., 2009, 2018a; Malkova, 2010*]. In the area of the Marre-Sale station, measurements of the methane content in the AL, permafrost and ground ice, and methane emission from the surface of predominant landscapes were performed. In the area of the Pechora River mouth, initial data on the CH_4 content in frozen and thawed sediments were obtained (Fig. 1).

The Marre-Sale Station

The Marre-Sale permafrost station is located near the weather station of the same name. The station belongs to the zone of typical tundra with maritime Arctic climate. According to the Marre-Sale weather station data, the mean annual air temperature (MAAT) from 1961 to 1990 (the period of the climatic norm) was –8.5°C. The coldest month is February with the mean monthly air temperature of –22.7°C; the warmest month is July (7.1°C). In recent decades (approximately since 1970), air temperature has been rising everywhere in the Arctic. In the studied region, the mean annual temperature has increased by about 2.8°C (1970–present), which is close to the "hard" scenario of climate change [*IPCC, 2018*]. The area belongs to the zone of continuous permafrost. Despite the presence of relatively homogeneous sandy or loamy sandy sediments in the upper part of the section, the AL depth varies from 0.3 to 2 m and more in dependence on the landscape conditions.

The landscape structure within the station area (Fig. 2) is representative of the typical tundra of Yamal Peninsula. The studied territory is located on the third marine terrace with heights from 15 to 30 m asl. The terrace is dissected by the system of ravines and runoff hollows and by deep (10–15 m) lake basins. The northern part of the territory is occupied by the wide floodplain of the Marre-Yakha River and by towpath and sea beach barrens. The floodplain is subdivided into low (regularly flooded, 0.1–0.5 m above the river water level), medium (periodically flooded, 0.5–1.5 m), and high (rarely flooded, >1.5 m) flood-

plain sections. The floodplain is boggy and contains numerous lakes occupying about 40% of the floodplain area. Flat areas between the lakes are occupied by polygonal herb-moss and dwarf shrub-herb-moss bogs. The total lake coverage is about 11% of the studied territory.

Herb-dwarf shrub-lichen tundras predominate on marine terraces; they are allocated to relatively drained positions between the lakes (sampling point BH6). Widespread herb-moss boggy lake depressions (point BH44) indicate the processes of active drainage of the lakes through runoff hollows. These two types of landscapes together occupy about 57% of the area, excluding the area of the lakes. Other landscape types almost equally occupy the remaining area (Fig. 2).

Hydrological conditions play an important role in the methane production in the active layer. The landscapes in the Marre-Sale area can be divided into four main classes according to their moisture content. The class of drained tundras includes sandy blowouts with fragments of tundra vegetation (point BH43) and drained polygonal tundra (point BH6).

The class of poorly drained tundras includes flat areas with wet surface covered by herb-dwarf shrub-lichen vegetation (point BH1) and the high floodplain of the Marre-Yakha River (point SB06). The class of wet tundras includes flat areas of wet herb-dwarf shrub-lichen-moss tundra (point BH3) and wet polygonal tundra with the herb-dwarf shrub-lichen-moss vegetation with small shallow ponds (points BH2, BH2a). The class of waterlogged tundras includes heavily moistened areas of ravines and runoff hollows (point BH4), lake basins (point BH44), polygonal herb-moss and dwarf shrub-moss areas of the low (point SB05) and medium (point BH36) floodplains of the Marre-Yakha River. The landscape of flat raised peatlands with the predomination of shrub-lichen-moss vegetation is distinguished separately.

The Pechora River mouth

In the European part of Russia (Nenets Autonomous District), field studies were conducted in the areas of three geocryological stations – Bolvansky, Kumzha, and Kashin – in the southern tundra subprovince of marine and alluvial accumulative plains.

The mean annual air temperature for the climatic norm period (1961–1990) is –4.7°C at the Cape Konstantinovsky weather station, which is the closest weather station to the study area. Over the last 15 years, the mean annual air temperature has risen to –2.7°C. The lowest mean annual air temperature (–9.1°C) over the entire observation period (since 1935) was recorded in 1998; and the highest mean annual air temperature (–0.7°C), in 2013. A general trend towards the mean annual air temperature rise by 0.06°C/yr has been observed in the past 30 years.

The Bolvansky station in the delta of the Pechora River on the southern coast of the Pechora Bay (the Barents Sea basin) within the gently hilly third marine plain raised at 25 to 35 m asl. The poorly drained spotty moss-lichen-dwarf shrub tundra on the tops and slopes of the hills predominates in this area. Surface sediments are represented by marine and coastal loamy sands and loams with interlayers and lenses of silty sands. Peat from 0.5 to 5 m in thickness occurs at the surface of polygonal peatlands and bogs. The territory of the station belongs to the area of continuous permafrost. Two pits were sampled at the Cape Bolvansky site. The first pit was located on the gently sloping surface of the polygonal waterlogged peatland (point 20P4). The second pit was excavated on a gently sloping surface of the polygon between runoff hollows within waterlogged peatland (point 20P6).

The Kashin geocryological station, 50 km west of the Bolvansky station, was established in 2009. It is found on Kashin Island in the Korovinskaya Bay of the Pechora River mouth, on the first marine terrace elevated at 2–10 m asl. Kashin Island is mostly com-

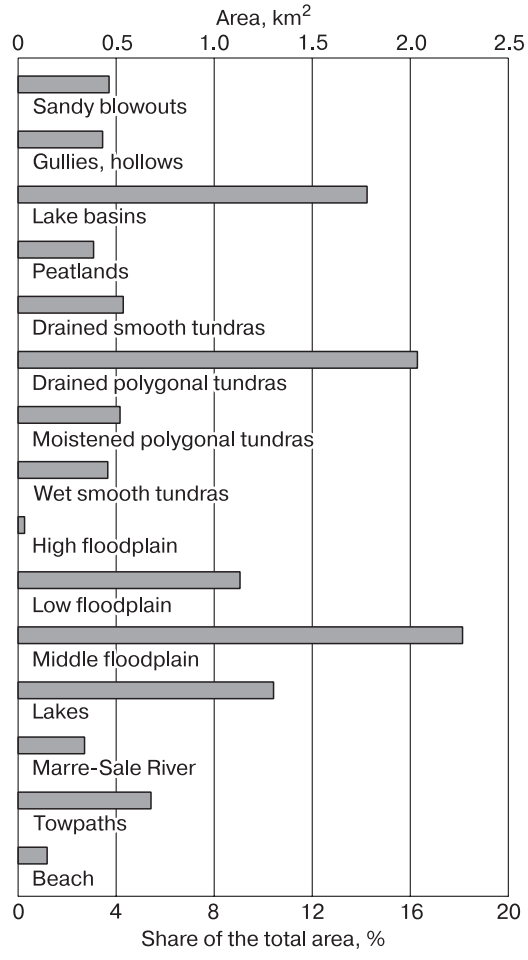

Fig. 2. Landscape structure of the Marre-Sale site.

posed of frozen sands covered with peat (up to 2 m in thickness) in some places. One pit and one exposure of the retreating coast were described and sampled. The pit was excavated on a gently inclined poorly drained surface with hillocky microtopography and lichen vegetation (point 20P3). The second sampling point was allocated to a polygonal peatland on the first alluvial–marine terrace elevated by about 1.6 m (point 20P7).

The Kumzha site was established 7 km to the south of Kashin Island, in the Pechora River delta-front, on a remnant of the first alluvial terrace at 5–8 m asl. Two pits were sampled. The first pit was laid on a slightly wavy drained surface flat-topped peatland with dwarf birch-lichen vegetation surrounded by waterlogged sedge-dominated depressions (point 20P1). The second pit was found in the central part of the depression (drained thermokarst lake) with sedge-sphagnum vegetation (point 20P2).

The Kashin and Kumzha sites belong to the zone of sporadic permafrost. The average depth of the active layer in the recent decades, according to data from CALM R24 (Bolvansky) and R24A (Kashin) sites, has been about 1.0–1.2 m.

METHODS

To determine the content of methane in frozen and thawed sediments, sediment samples of about 50 cm^3 were taken and placed in 150-mL plastic syringes after weighing. The samples were degassed using the Head Space method [*Kampbell et al., 1989*]. A highly concentrated NaCl solution and air of the known volume (about 50 cm^3) were pumped into the syringe. After complete thawing of the sample, emitted gas was pumped from the syringe into sealed 10-mL glass test-tubes with rubber corks. The samples were transported to the laboratory of the VNIIOkeangeologiya, where the gas composition was determined by gas chromatography on the SHIMADZU GC 2014 (Japan) flame ionization detector.

To determine the water content, the samples were taken in parallel with the samples for the gas composition determination.

In the late July and early August 2018, 2019, and 2020, CH_4 specific fluxes were measured in predominant landscapes in the Marre-Sale area. Isolated cubic chambers of 25 × 25 × 25 cm made of acrylic glass were used for measurements. Inside the chambers, air was automatically stirred for 15 s by fans every 10 min. Two-channel loggers HOBO Pro v2 (USA) with sensors on the surface (in a layer of the vegetation cover) and at a depth of 10 cm were installed near the chambers to measure temperature. Accuracy of the logger measurements was ±0.1°C.

Temperature was recorded every 10 min. Gas was sampled after the beginning of the experiment every hour during four hours (i.e., five measurements) by a 150-mL plastic syringe from the center of the chamber; then, gas was immediately pumped into 10-mL sealed glass test-tubes. The samples were analyzed in the laboratory of the VNIIOkeangeologiya with the use of the above-mentioned instrument. The CH_4 specific fluxes were further calculated from the slope of linear trends of the CH_4 concentration in mg/(m^2·h) taking into consideration changes in the temperature and air pressure during the experiment [*Glagolev et al., 2010*].

Data on the CH_4 concentration in sediments and ice and on the CH_4 emission were analyzed by standard statistical methods. All data were sorted into groups according to their geological and genetic background or according to the landscape characteristics of sampling sites. Mean, minimum, maximum, standard deviation, and median values were calculated for the analyzed statistical samples. The results were presented in graphs, diagrams, and figures. In box plot diagrams, the lower and upper edges of a rectangle ("box") correspond to the first and third quartiles of the sample. The crosses in each field represent the mean methane content. The ends of the "whiskers" are the edges of a statistically significant selection (the lower end is the difference of the first quartile and one and a half interquartile distance; the upper end is the sum of the third quartile and one and a half interquartile distance). Dots on the box plot diagram designate the values of the methane content or methane flux.

RESULTS AND DISCUSSION

The methane content in the active layer and upper permafrost horizon

The methane content in the AL (regardless of the AL thickness in different years) and in the upper permafrost horizon (UPH) (to a depth of 3.6 m) in the Marre-Sale station area have been studied annually since 2012. Overall, 369 samples have been analyzed, including 249 samples in the thawed state and 120 samples in the frozen state. For the Pechora River mouth, 42 samples were taken (11 samples in the frozen state, 31 in the thawed state). The methane content was not studied in peat bogs, the Marre-Yakha River towpaths, and on the sea beach. The methane content in such areas is low due to the unfavorable conditions for significant methanogenesis [*Kwon et al., 2017*].

Figure 3 demonstrates sediment sections obtained from shallow (up to 3.6 m) boreholes: composition of the sediments, total weight water content, and the methane content in AL and UPH in different years for the area of the Marre-Sale station.

Against the background of considerable variability in the methane content in the AL, in general, there is a natural increase in the CH_4 content with depth. This probably indicates an important role of diffusion

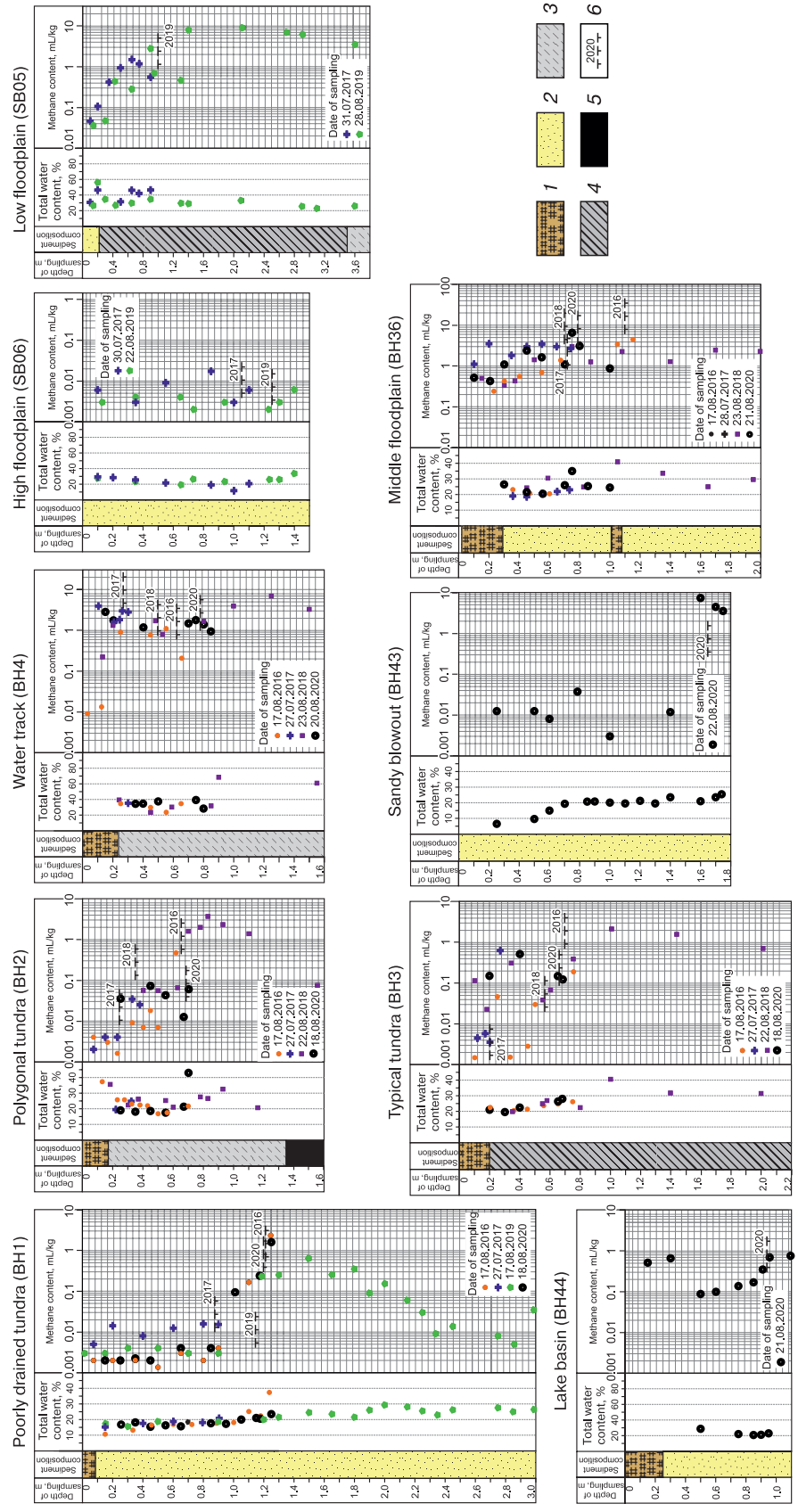

Fig. 3. Change in the methane content with depth in different types of landscapes in the Marre-Sale area.

1 – peat, *2* – sand, *3* – loamy sand, *4* – loam, *5* – ice with mineral admixtures (probably, wedge ice), *6* – boundary of the active layer at the time of drilling and the year of sampling.

mechanism of methane transfer to the surface. The amount of methane in the UPH is always higher than in the AL. The highest methane contents in both AL and UPH are typical for the most waterlogged sedge-dominated landscapes. The diffusion mechanism of the methane distribution in the AL may indicate the strong influence of methanotrophic bacteria that use methane as the only source of carbon and energy. As a rule, aerobic layers, where methanotrophic bacteria develop, are located above anaerobic zones of the methanogenesis [*Whalen, Reeburgh, 1990*].

Figure 4 demonstrates the statistical data on the CH_4 content in the AL and UPH at the Marre-Sale area. It can be seen that the CH_4 content varies considerably in dependence on a landscape. The ratio of the average CH_4 content in the landscapes with the maximum CH_4 contents to that in the landscapes with the minimum CH_4 contents is up to 400. Differences in the amount of methane are significant for the samples both from the AL and from the UPH.

In the Marre-Sale area, the highest methane content in the AL was observed in the middle floodplain of the river (point BH36) and averaged 1.59 ± 1.36 mL/kg with the maximum of 6.55 mL/kg. Almost the same values (1.57 ± 2.62 with the maximum of 9.05 mL/kg) were obtained for the low floodplain. On the main surface of the third marine terrace, the highest methane content in the AL was obtained for the moistened surface of the runoff hollows (point BH4) and averaged 1.54 ± 1.09 mL/kg with the maximum of 3.93 mL/kg. The high values of the methane content in AL were recorded in polygonal tundra (points BH2, BH2a). All other landscapes were characterized by much lower methane contents in thawed sediments (Fig. 4). In the moist typical tundra (point BH3), the average methane content was 0.13 ± 0.18 mL/kg; in point BH44 (lake basin), it was 0.28 ± 0.23 mL/kg. The methane content was less than 0.1 mL/kg in the AL of the moist flat tundra (point BH1), in drained sandy blowouts (point BH43), and in the high floodplain of the Marre-Yakha River (point SB06). On the basis of the obtained data, it can be assumed that there is a definite tendency for an increase in the methane content with an increase in the degree of surface moistening and in the water content of the AL; however, this relationship is not linear and is not observed over the entire area.

In all cases, the methane content in the UPH is higher than in the AL (Fig. 4). The difference in the ratio of the methane content in the UPH to the methane content in the AL for different types of landscapes is significant and ranges from 130–150 to 500–600% and higher. The maximum methane contents are observed near the upper permafrost horizon and 0.3–0.5 m deeper than the maximum thickness of the AL. Below, the methane content gradually decreases down the section. The similar distribution of methane was previously established for the sections in the northeastern Siberia [*Kraev, Rivkina, 2017*].

In general, the high methane contents in the UPH were obtained for sampling points BH43, BH36, BH4, BH2a, and SB05, i.e., for the same landscapes, where the high methane content was observed in the AL. In a single case (point BH43, drained surface of a sandy blowout), the high methane content values were obtained for the underlying frozen sediments (the average methane content 5.14 ± 1.9 mL/kg with the maximum value of 7.29 mL/kg), though in the AL, the methane content was exceptionally low. This can be explained by a high degree of drainage of the upper sandy horizon, which does not provide the anaerobic conditions and the methane formation.

In the area of the Pechora River mouth, the CH_4 content was determined at the sites within several landscape structures (Fig. 5).

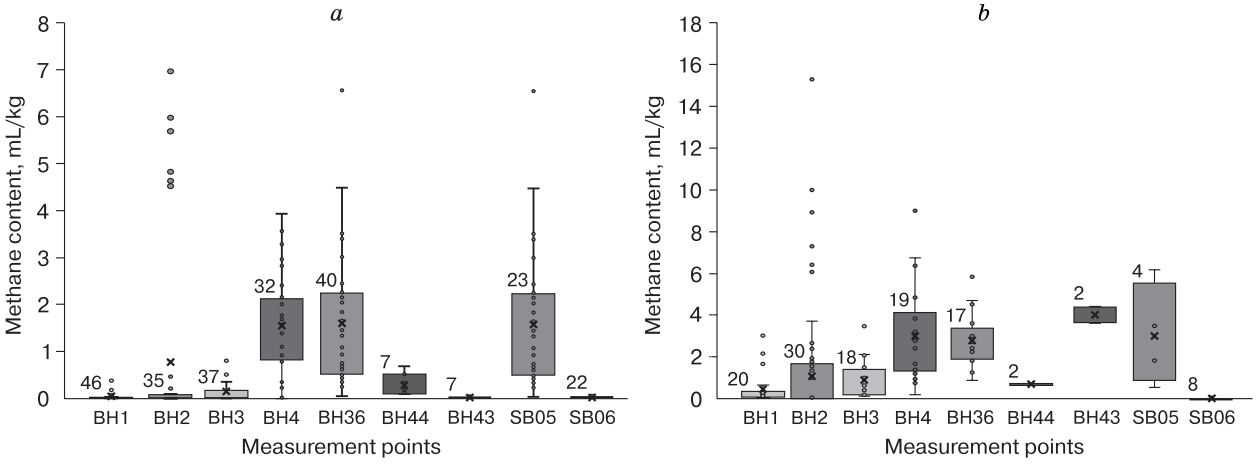

Fig. 4. Box-plot diagrams of the methane content at observation points in the Marre-Sale area in the (*a*) active layer and (*b*) upper permafrost horizon.

Figures indicate the number of samples.

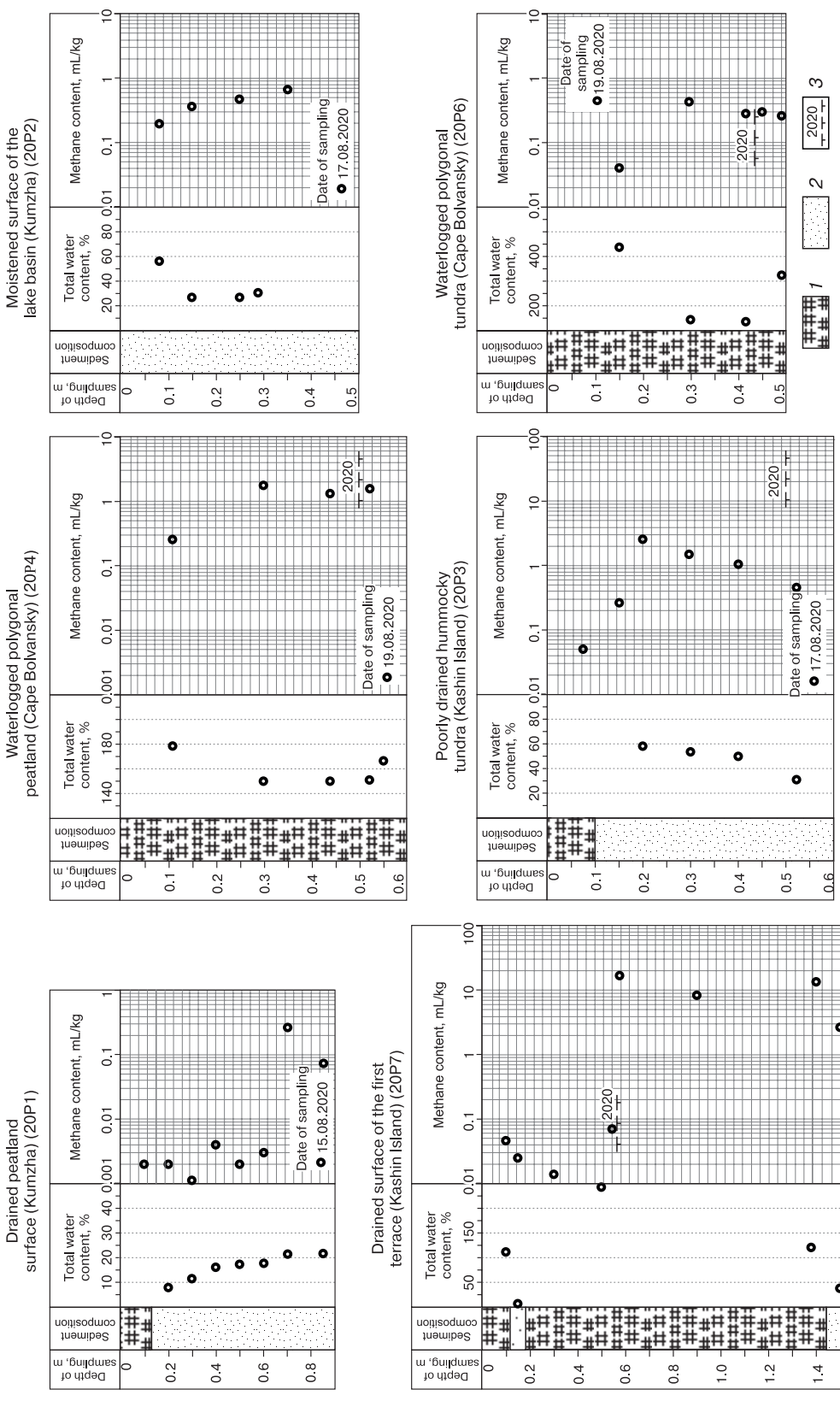

Fig. 5. Changes in the methane content by depth in different types of landscapes near the mouth of the Pechora River.

1 – peat; *2* – sand; *3* – boundary of the active layer at the time of drilling and the year of sampling.

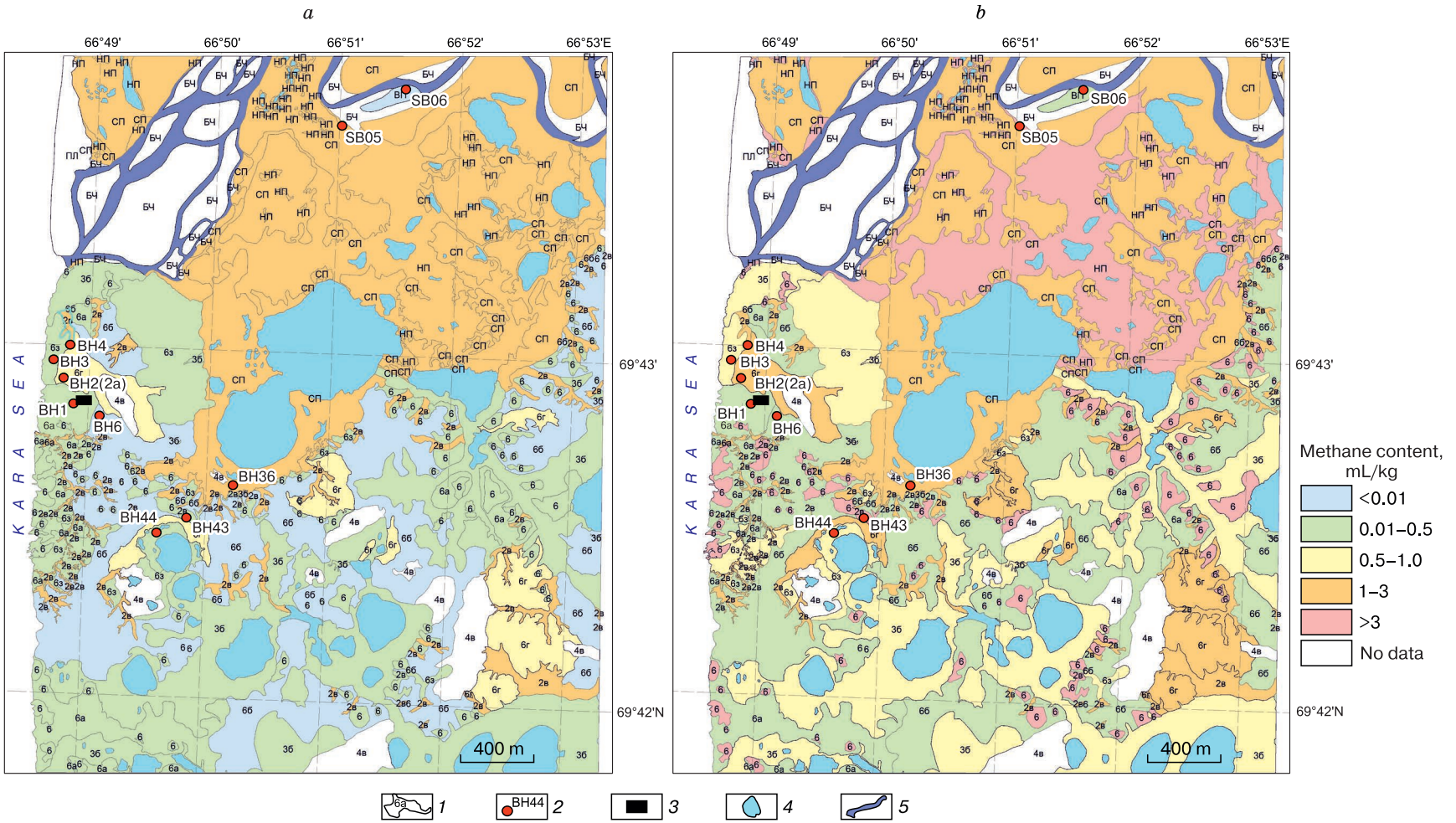

Fig. 6. Maps of the average methane content in the predominant landscapes of the Marre-Sale area in the (*a*) thawed sediments of the active layer and (*b*) upper permafrost horizon.

1 – landscape boundary and index (2с(2в) – gullies and water tracks, 3b(3б) – lake basins, 4c(4в) – peatlands, 6 – sandy blowouts, 6a(6а) – drained smooth tundras, 6b(6б) – drained polygonal tundras, 6d(6г) – waterlogged polygonal tundras, 6z(6з) – wet smooth tundras, LF(НП) – low floodplain, MF(СП) – middle floodplain, HF(ВП) – high floodplain, SB(ПЛ) – sea beach, TP(БЧ) – unvegetated zones between floodplain and seashore (towpaths)); *2* – sampling point and its index; *3* – Marre-Sale weather station; *4* – lakes; *5* – Marre-Yakha River.

The high methane content in thawed sediments of the AL near the Pechora River mouth was recorded at sampling sites 20P3 and 20P4; the average CH_4 contents were 1.24 ± 1.08 mL/kg (maximum 2.5 mL/kg) and 1.1 ± 0.83 mL/kg (maximum 1.9 mL/kg), respectively. At point 20P2, the average methane content in the AL was 0.42 ± 0.2 mL/kg (maximum 0.67 mL/kg); at point 20P6, the average value was 0.24 ± 0.19 mL/kg (maximum 0.41 mL/kg). At points 20P1 and 20P7, the CH_4 concentrations were insignificant, less than 0.05 mL/kg. The given data, as well as the data for the Marre-Sale territory, indicate some increase in the amount of CH_4 in the more moistened landscapes compared to the drained surfaces.

Frozen sediments in the UPH were sampled at points 20P3, 20P4, 20P6, 20P7. The CH_4 content in them was higher than in the AL for all points, except for 20P3. The maximum values were obtained for frozen sediments in the coastal cliff on Kashin Island (point 20P7); they average CH_4 content was 8.15 ± 6.14 mL/kg (maximum 15.78 mL/kg). In other points, the average methane content comprised 1.68 mL/kg (20P4), 0.46 mL/kg (20P3), 0.3 mL/kg (20P6).

The maps illustrating the spatial distribution of methane in the AL and UPH are presented in Fig. 6. The earlier created landscape map of the study area [*Oblogov et al., 2020*] was used as the base map. To show the methane content in sediments, average data obtained at sampling points were sorted into five unequal gradations shown by color on the map.

The maps clearly illustrate the spatial distribution of methane in the AL and UPH and allow us to estimate the amount of methane that will be emitted into the atmosphere for different scenarios of climatic warming and permafrost degradation under the typical tundra conditions.

Methane in permafrost and ground ice of the Marre-Sale Area

Data on the methane content in the Quaternary permafrost and ground ice of the Marre-Sale area were obtained by studying coastal cliffs of 10 to 30 m in height (Fig. 7) [*Kanevskii et al., 2005; Streletskaya et al., 2009, 2018a*].

In the upper part of the section, fine-grained alluvial sands of the Holocene age (aIV) are exposed. They have the lowest CH_4 content among all geological varieties; the average value is 0.08 ± 0.1 mL/kg; the maximum value is 0.35 mL/kg.

Continental layered silty loamy sands and sands of lacustrine-bog ($lbIII^4$) or coastal-marine ($amIII^{3-4}$) origin underlie Holocene sands. The CH_4 content in these sediments is an order of magnitude higher than in the Holocene sands; it averages 0.87 ± 1.13 mL/kg with a maximum of 3.81 mL/kg.

Loamy sands and sands ($amIII^{3-4}$) were formed within the vast coastal plain with numerous lakes [*Streletskaya et al., 2009*]. These sediments are characterized by the high variability in the CH_4 content, with the maximum value of 6.75 mL/kg and the average value of 0.46 ± 1.16 mL/kg.

The base of the section is composed of clay and loamy sediments with interlayers of sands of the Late Pleistocene age ($mIII^1$) of the marine and coastal-marine origin. The silty clay sediments are most enriched in CH_4 content: 1.94 ± 1.62 mL/kg (average) and 6.77 mL/kg (maximum).

The am III^{3-4} sediments in the middle part of the section contain subhorizontal lenses and interlayers of ice with wave-like bends and single mineral inclusions. The pure ice layers with a thickness from a few centimeters to 1.5 m (0.2–0.5 m on average) alternate with sandy (loamy sandy) interlayers. The ice contains irregularly distributed bubbles, 1–2 mm in diameter of a rounded or poorly elongated shape, in

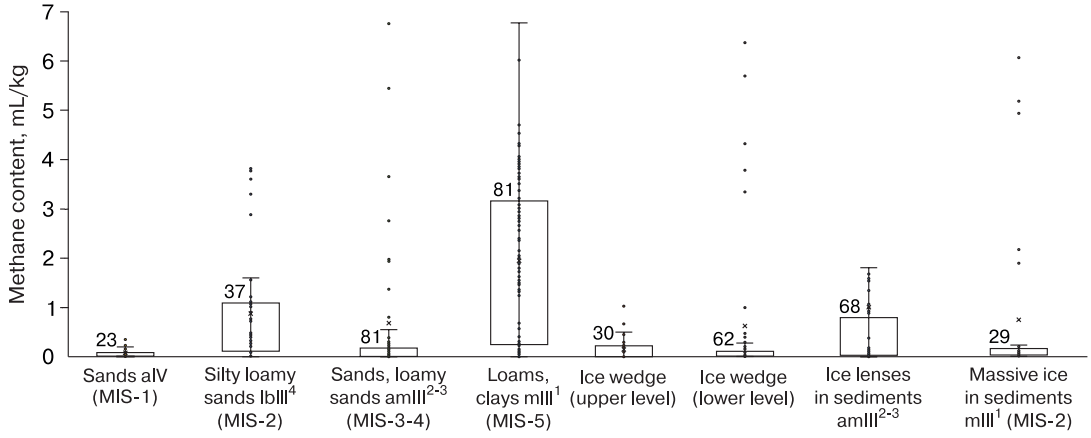

Fig. 7. Box-plot diagrams of the methane content in the Quaternary frozen sediments and ground ice in the area of the Marre-Sale coastal cliff.

Figures indicate the number of samples.

which gas occurs under pressure. The amIII$^{3-4}$ sequence of sandy sediments with inclusions of ice lenses and interlayers is visually seen as a single ice-rich horizon and is united into the horizon of massive ice of the first type (MI 1). The ice lenses contain the significant amount of methane. The average methane content is 0.98 ± 3.25 mL/kg. The absolute maximum is 23.29 mL/kg was determined in a sample from the ice lens in the amIII$^{3-4}$ sediments. This is the maximum value among all sampled sediments.

Thick massive ice of the second type (MI 2) is exposed 3.0–3.5 km to the south of the polar station in the thickness of the mIII^{1} loamy clay sediments. The apparent thickness of the ice body is more than 8 m; the lower part descends under sea level. The ice is almost clear and glassy, but there are zones with a significant number of admixtures of mineral inclusions (mainly clayey and silty fractions) in the form of suspended matter. Ice includes small irregularly distributed gas bubbles and their clusters. Gas in the bubbles is under pressure. The average methane content in the MI 2 samples is 0.76 ± 1.69 mL/kg; the maximum reaches 6.07 mL/kg.

There are two generations of ice wedges (IW) in the section. The Holocene IW of the upper level is distinctly wedge-shaped and often superimposes the lower-level of older wedges. The wedges with a width of 0.5–1.2 m at the top and 1.0–3.5 m in height form a polygonal network; the size of polygon sides is 6–8 m. The wedges are of the syngenetic type of growth, as indicated by the relatively high ice content of host sands and peat. Wedge ice contains numerous vertically oriented gas bubbles of up to 3 mm in size. The average methane content in the samples of IW of the Holocene age is 0.15 ± 0.24 mL/kg; the maximum value is 1.03 mL/kg.

Large ice wedges began to form at the end of MIS-3 (Marine Isotope Stage 3) and continued active growth in MIS-2 [*Forman et al., 2002*]. The wedges of 1.5–4.0 m in width and up to 10 m in height form a polygonal network of 10–20 m in size. The wedges are syngenetic, as indicated, in particular, by the repeatedly encountered layered cryogenic structure of the host sediments. The wedge tails in the central part of the coastal cliff are involved in the MI 1 massif, branching and bending in different directions. The IW is transparent, with thin vertically oriented interlayers of mineral inclusions of sandy silt fraction. Numerous gas bubbles 0.1–2.0 mm in size extend vertically in the ice. The average methane content of the Pleistocene IW samples is 0.63 ± 1.89 mL/kg, with the maximum value of 11.11 mL/kg.

The CH_4 concentrations within the same geological and genetic variety can differ by several orders

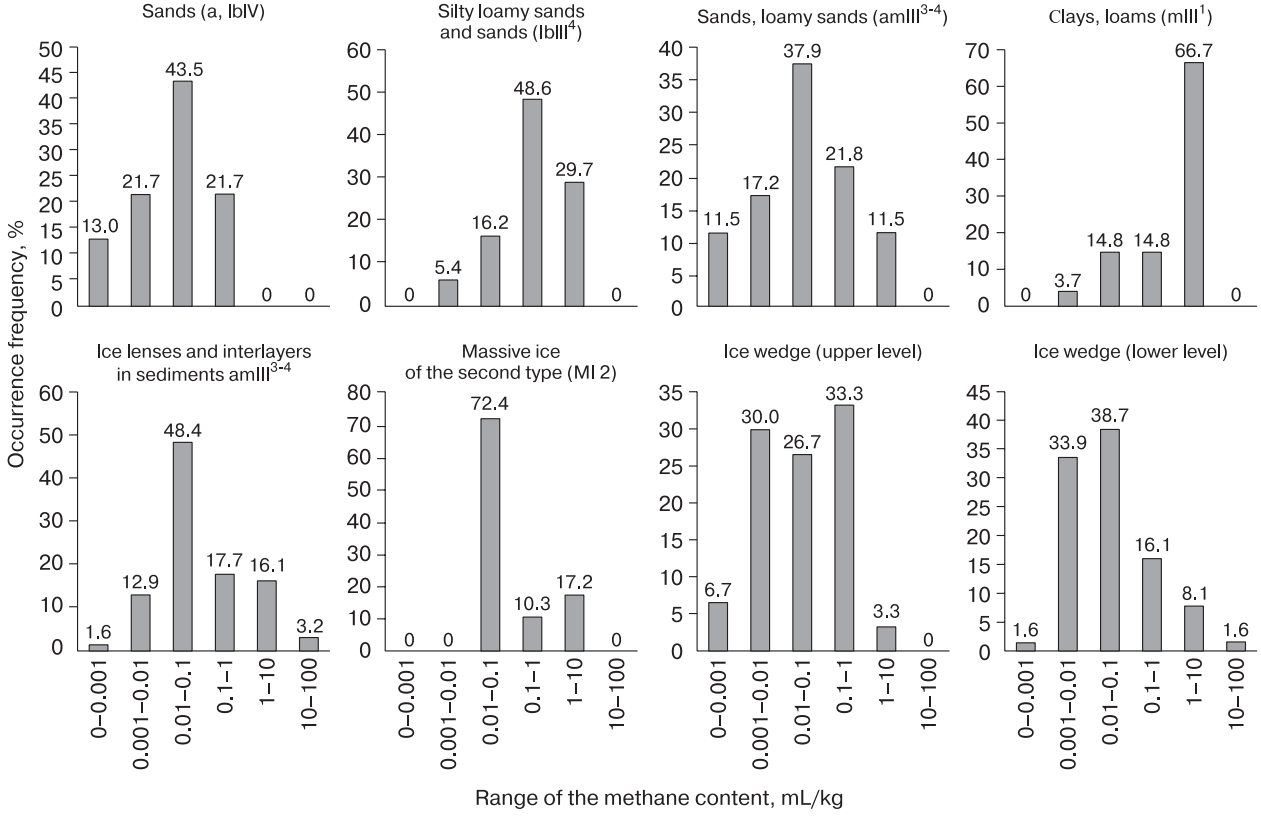

Fig. 8. Methane contents in different genetic types of frozen sediments and ground ice in the Marre-Sale area.

of magnitude, in dependence on the place of sampling. This is primarily relevant to massive ice areas, where completely different values were obtained in samples taken within a few tens of centimeters from one another. Figure 8 demonstrates the distributions of the CH_4 content in the Quaternary frozen sediments and ground ice in the Marre-Sale area.

It is evident that in most of the considered geological-genetic varieties, the pattern of the CH_4 distribution is close to the lognormal one. In general, the maximum values range from 0.01 to 0.10 mL/kg. Significant deviations from the lognormal distribution are observed only for marine loamy clay sediments mIII[1], where the values ranging from 1 to 10 mL/kg distinctly predominate, and for MI 2, where the range of 0.01 to 0.10 mL/kg predominates.

The obtained data point to the high methane content in the Quaternary permafrost and ground ice. Nevertheless, each geological and genetic type is characterized by its own methane content indicating the influence of the conditions of sediment deposition and freezing. Thus, methane can act as an additional indicator for geocryological subdivision of frozen sediments.

Emission of methane from the surface of the predominant landscapes of Marre-Sale

The specific CH_4 efflux to the atmosphere (methane emission) was measured in the Marre-Sale area in the late July – early August in 2018, 2019, and 2020 at nine key points (BH1, BH2, BH2a, BH3, BH4, BH36, BH44, SB05, SB06) within eight dominant landscapes.

The measurements were not performed in peatlands, drained surface of sandy blowouts, Marre-Yakha River towpath, and the sea beach. For similar types of landscapes, it was previously established that methane efflux is virtually absent [*Kwon et al., 2017*].

Twenty six four-hour experiments were conducted at the surface temperatures from 5.7 to 20.0°C.

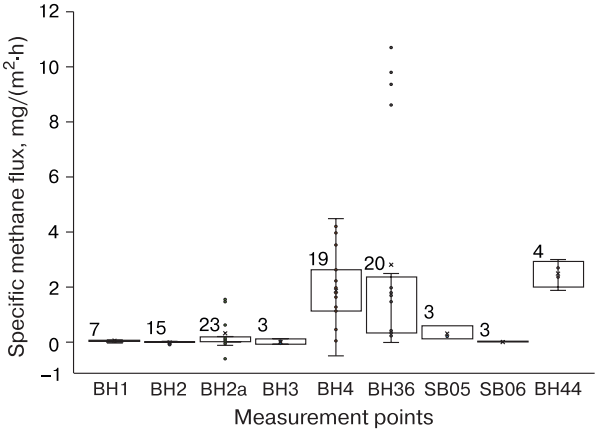

Fig. 9. Box-plot diagrams of the specific methane flux from predominant landscapes of Marre-Sale area.

Figures indicate the number of samples.

Figure 9 demonstrates the results of the measurements.

There are several types of landscapes with high positive values of the specific methane fluxes. These are the waterlogged floodplain (points BH36 and SB05), the heavily moistened runoff hollows (point BH4), the waterlogged surface of the lake basin (point BH44), and the highly moistened surface of the polygonal depression (point BH2a). The maximum value of the specific methane flux (10.7 mg/(m²·h) was obtained in point BH36 at the surface temperature of 20.0°C. In point BH4, the maximum methane flux was 4.5 mg/(m²·h) at the surface temperature of 16.9°C; in point BH44, these values were 2.99 mg/(m²·h) and 17.1°C, respectively. The greatest methane flux at point BH2a (1.5 mg/(m²·h)) was obtained at the surface temperature of 13.1°C. In other points, the specific flux values were always less than 0.1 mg/(m²·h). Approximately the same methane fluxes were measured earlier in various ecosystems of Alaska in the zone of continuous permafrost [*Euskirchen et al., 2017*].

The relationship between the specific methane fluxes and the surface temperature at the time of sampling clearly demonstrates a tendency for the increase in the methane fluxes with a rise in the surface temperature (Fig. 10). This is best manifested for the landscapes with large methane fluxes. In particular, at

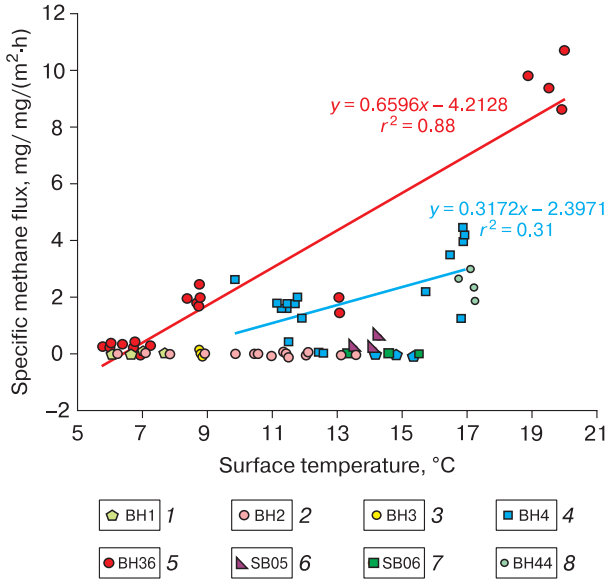

Fig. 10. The relationship between the specific methane fluxes and the surface temperature at measurement points in the predominant landscapes of the Marre-Sale area.

1–8 – measurement points (*1* – drained smooth tundra, *2* – drained polygonal tundra, *3* – wet smooth tundra, *4* – runoff hollow, *5* – middle floodplain, *6* – low floodplain, *7* – high floodplain, *8* – lake basin). Linear trends are presented for some data sequences.

point BH36, we can distinguish three temperature ranges, at which we measured the methane fluxes. At the surface temperature of 5.7 to 7.2°C, the lowest methane flux close to zero or negative was observed. At the surface temperature of 8–9°C, the methane flux increased significantly and reached 1.68–2.47 mg/(m^2·h). The highest methane flux of 8.6–10.7 mg/(m^2·h) at point BH36 was obtained at the surface temperatures from 18.8 to 20.0°C.

CONCLUSIONS

As a result of the studies conducted in the Marre-Sale area, new statistically reliable data on the methane content in the AL and the underlying UPH (transient and intermediate permafrost layers) were obtained.

In Marre-Sale, the highest methane content in the AL was recorded in the waterlogged landscapes of the middle and low floodplains; it averaged 1.59 ± 1.36 and 1.57 ± 2.62 mL/kg, respectively. For the third marine terrace, the high methane content in the AL was obtained for the waterlogged runoff hollows and for the polygonal tundra. In well-drained landscapes (drained surface of typical tundra, sandy blowouts, etc.), the lowest methane content in the AL was observed. A typical increase in the CH_4 content with depth in the AL probably indicates an important role of methane diffusion to the surface.

In the UPH sediments, the methane content is up to 5–6 times higher than in the AL and averaged 3 mL/kg. The high methane content in the UPH was obtained for the landscapes, in which the high methane content was also observed in the AL. The high CH_4 content in the UPH is explained by penetration of methane into the underlying layers during the autumn freezing of the AL.

The transient layer of permafrost with the high content of methane can be considered as a significant potential source of methane, which may be involved in the turnover of greenhouse gases in the atmosphere during the permafrost degradation.

The content and distribution of methane in various geological and genetic types of the Quaternary permafrost and ground ice of different origins in the Marre-Sale area were analyzed. The highest methane concentrations were found in the loamy clay sediments of marine origin ($mIII^1$) (on average, about 2 mL/kg with a maximum of 6.77 mL/kg). These sediments occur at the base of the section and constitute a larger part of the sediments exposed in the coastal cliff. High methane contents were also established for ground ice of the area. The absolute maximum of the methane content (23.29 mL/kg) was obtained in the interlayers and lenses of glassy ice in the alluvial-marine (coastal-marine) sandy loams and sands ($amIII^{3-4}$); although, in this type of ice, the average methane content did not exceed 1 mL/kg. It was shown that the methane content within the same genetic type of sediments can differ by several orders of magnitude in dependence on the local conditions of particular sampling sites. The methane distribution pattern for most of the distinguished genetic types of frozen sediments and ground ice is close to lognormal.

The peak values of the specific methane fluxes into the atmosphere from the surface of typical tundra landscapes in the Marre-Sale area were determined. Stable and significant methane fluxes were observed for the waterlogged surface of the low and middle floodplains, waterlogged runoff hollows, waterlogged surfaces of lake basins, and highly moistened surfaces of polygonal depressions. The maximum value of methane flux (10.7 mg/(m^2·h)) was obtained on the middle floodplain at the surface temperature of about 20.0°C. On the surfaces of the poorly moistened and drained landscapes, the specific methane fluxes are always less than 0.1 mg/(m^2·h). Taking into consideration the landscape structure of the Marre-Sale area, the sources of significant methane emissions occupy 45–50% of the territory.

Acknowledgments. *This work was supported by the Russian Science Foundation (grant no. 22-27-00181). Cryolithological studies were conducted within the framework of the Development Program of the Interdisciplinary Research and Education School at Lomonosov Moscow State University "The Future of the Planet and Global Environmental Change" and state assignment no. 121051100164 "Evolution of the Cryosphere under Climate Change and Human Impact".*

References

Anisimov O.A., 2007. Potential feedback of thawing permafrost to the global climate system through methane emission. *Environ. Res. Lett.* **2**, 1–7. DOI: 10.1088/1748-9326/2/4/045016.

Anthony K.W., von Deimling T.S., Nitze I. et al., 2018. 21st-century modeled permafrost carbon emissions accelerated by abrupt thaw beneath lakes. *Nat. Commun.* **9**, 3262. DOI: 10.1038/s41467-018-05738-9.

Christensen T.R., 2014. Understand Arctic methane variability. *Nature* **509**, 279–281. DOI: 10.1038/509279a.

Ciais P., Sabine H.C., Bala G. et al., 2013. Carbon and Other Biogeochemical Cycles. In: *Climate Change 2013: The Physical Science Basis. Contribution of Working Group I to the Fifth Assessment Report of the Intergovernmental Panel on Climate Change* [T.F. Stocker, D. Qin, G.-K. Plattner, M. Tignor, S.K. Allen, J. Boschung, A. Nauels, Y. Xia, V. Bex, P.M. Midgley (eds.)]. Cambridge, UK and NY, USA, Cambridge Univ. Press, pp. 465–570.

Dean J.F., Middelburg J.J., Röckmann T. et al., 2018. Methane feedbacks to the global climate system in a warmer world. *Rev. Geophys.* **56**, 207–250. DOI: 10.1002/2017RG000559.

Euskirchen E.S., Bret-Harte M.S., Shaver G.R. et al., 2017. Long-Term Release of Carbon Dioxide from Arctic Tundra Ecosystems in Alaska. *Ecosystems* **20**, 960–974. DOI: 10.1007/ s10021-016-0085-9.

Forman S.L., Ingolfsson O., Gataullin V. et al., 2002. Late Quaternary stratigraphy, glacial limits and paleoenvironments of Maresale area, western Yamal Peninsula, Russia. *Quatern. Res.* **21**, 1–12.

French H., Shur Y., 2010. The principles of cryostratigraphy. *Earth Sci. Rev.* **101** (3–4), 190–206. DOI: 10.1016/ j.earscirev.2010.04.002.

Glagolev M.V., Sabrekov A.F., Kazantsev V.S., 2010. *Measurement of Gas Exchange at the Soil / Atmosphere Boundary*. Tomsk, Tomsk State Pedagogical Univ., 96 pp. (in Russian).

IPCC, 2018. Global Warming of 1.5°C. An IPCC special report on the impacts of global warming of 1.5°C above preindustrial levels and related global greenhouse gas emission pathways. In: *The Context of Strengthening. The Global Response to the Threat of Climate Change, Sustainable Development, and Efforts to Eradicate Poverty.* V. Masson-Delmotte, P. Zhai, H.-O. Pörtner et al. (Eds.). Cambridge, New York, Ridge Univ. Press, 616 pp. DOI: 10.1017/9781009157940.

Kampbell D.H., Wilson J.T., Vandegrift S.A, 1989. Dissolved oxygen and methane in water by a GC Headspace Equilibration Technique. *Intern. J. Environ. Analytic. Chemistry* **36** (4), 249–257. DOI: 10.1080/03067318908026878.

Kanevsky M.Z., Streletskaya I.D., Vasiliev A.A., 2005. Formation of cryogenic structure of Quaternary sediments in Western Yamal (by the example of Marre-Sale area). *Kriosfera Zemli* **9** (3), 16–27 (in Russian).

Kraev G.N., Rivkina E.M., 2017. Accumulation of methane in freezing and frozen soils of the permafrost zone. *Arctic Environ. Res.* **17** (3), 173–184. DOI: 10.17238/issn2541-8416.2017.17.3.173 (in Russian).

Kraev G., Schulze E.-D., Yurova A. et al., 2017. Cryogenic displacement and accumulation of biogenic methane in frozen soils. *Atmosphere* **8** (6), 105. DOI: 10.3390/at-mos8060105.

Kraev G.N., Schulze E.-D., Rivkina E.M., 2013. Cryogenesis as a factor in the distribution of methane in frozen horizons. *Dokl. Akad. Nauk* **451** (6), 684–687 (in Russian).

Kwon M.J., Beuli F., Ilie I. et al., 2017. Plants, microorganisms, and soil temperatures contribute to a decrease in methane fluxes on a drained Arctic floodplain. *Glob. Chang. Biol.* **23**, 2396–2412. DOI: 10.1111/gcb.13558.

Malkova G.V., 2010. Mean-annual ground temperature monitoring on the steady-state-station "Bolvansky". *Kriosfera Zemli* **14** (3), 3–14 (in Russian).

McCalley C., Woodcroft B., Hodgkins S. et al., 2014. Methane dynamics regulated by microbial community response to permafrost thaw. *Nature* **514**, 478–481. DOI: 10.1038/nature13798.

McGuire A.D., Christensen T.R., Hayes D. et al., 2012. An assessment of the carbon balance of Arctic tundra: comparisons among observations, process models, and atmospheric inversions. *Biogeosciences* **9**, 3185–3204. DOI: 10.5194/bg-9-3185-2012.

Oblogov G.E., Vasiliev A.A., Streletskaya I.D. et al., 2020. Methane content and emission in the permafrost landscapes of Western Yamal, Russian Arctic. *Geosciences* **10** (10), 412. DOI: 10.3390/geosciences10100412.

Pavlov A.V., Anan'eva G.V., Drozdov D.S. et al., 2002. Monitoring of active layer and the temperature of frozen grounds in the north of Russia. *Kriosfera Zemli* **6** (4), 30–39 (in Russian).

Rivkina E.M., Samarkin V.A., Gilichinskiy D.A., 1992. Methane in permafrost of the Kolyma-Indigirka Lowland. *Dokl. Ross. Akad. Nauk* **323** (3), 559–562 (in Russian).

Sachs T., Giebels M., Wille C. et al., 2008. Methane emission from Siberian wet polygonal tundra on multiple spatial scales: Vertical flux measurements by closed chambers and eddy covariance, Samoylov Island, Lena River Delta. In: *Proc. 9th Intern. Conf. Permafrost* (Fairbanks, Alaska, 29 June–3 July, 2008), Fairbanks, pp. 1549–1554.

Schuur E.A.G., McGuire A.D., Schädel C. et al., 2015. Climate change and the permafrost carbon feedback. *Nature* **520**, 171–179. DOI: 10.1038/nature14338.

Streletskaya I.D., Shpolyanskaya N.A., Kritsuk L.N. et al., 2009. Cenozoic deposits of Western Yamal and the problem of their genesis. *Byull. Mosk. Gos. Univ., Ser. 5 (Geogr.)*, no. 3, 50–57 (in Russian).

Streletskaya I.D., Vasiliev A.A., Oblogov G.E. et al., 2018a. Methane in underground ice and frozen sediments on the coast and shelf of the Kara Sea. *Led i Sneg* **58** (1), 65–77. DOI: 10.15356/2076-6734-2018-1-65-77 (in Russian).

Streletskaya I.D., Vasiliev A.A., Oblogov G.E. et al., 2018b. Methane content in ground ice and sediments of the Kara Sea Coast. *Geosciences* **8** (12), 434. DOI: 10.3390/geosciences8120434.

Sturtevant C.S., Oechel W.C., Zona D. et al., 2012. Soil moisture control over autumn season methane flux, Arctic Coastal Plain of Alaska. *Biogeosciences* **9**, 1423–1440. DOI: 10.5194/bg-9-1423-2012.

van Huissteden J., 2020. *Thawing Permafrost: Permafrost Carbon in a Warming Arctic*. Springer Nature Switzerland AG, Cham, Switzerland, 508 pp. DOI: 10.1007/978-3-030-31379-1.

Walz J., Knoblauch C., Böhme L. et al., 2017. Regulation of soil organic matter decomposition in permafrost affected Siberian tundra soils – Impact of oxygen availability, freezing and thawing, temperature, and labile organic matter. *Soil Biol. Biochem.* **110**, 34–43. DOI: 10.1016/j.soil- bio.2017.03.001.

Whalen S., Reeburgh W., 1990. Consumption of atmospheric methane by tundra soils. *Nature* **346**, 160–162. DOI: 10.1038/346160a0.

Received December 20, 2021
Revised May 25, 2022
Accepted September 13, 2022

Translated by V.A. Krutikova